Thermal fluctuations of individual semiflexible polymers in confined geometry

Sarah Köster[1,2], Stephan Herminghaus[1,2], Jan Kierfeld[3], Holger Stark[4] and Thomas Pfohl[1,2*]

[1]Department of Applied Physics, University of Ulm, Germany
[2]Max Planck Institute for Dynamics and Self-Organization, Göttingen, Germany
[3]Max Planck Institute of Colloids and Interfaces, Potsdam, Germany
[4]Department of Physics, University of Konstanz, Germany

Abstract

Thermal fluctuations of individual actin filaments confined in rectangular microchannels with dimensions similar to the mesh size of the cytoskeleton in eukaryotic cells were studied using fluorescence microscopy. We observed a strong dependence of the tangent correlation on both channel width and filament length. Compared to freely fluctuating filaments, long filaments confined in narrow channels exhibit an enhanced tangent correlation with a local minimum. These unique characteristics may be described by an analytical expression assuming the confining energy as a parabolic potential. We find the $d^{2/3}$ law for the deflection length λ, which has been theoretically predicted for circular tubes and a hard wall potential, experimentally confirmed.

Introduction

Actin is among the most abundant proteins in the eukaryotic cell. A dense network of actin filaments (F-actin) regulates numerous crucial cellular processes such as cell motility, division, and shape. Furthermore, it is one of the principal components of the cytoskeleton and therefore responsible for the mechanical stability of the cell. Thus, the mechanical and dynamic properties of actin and its supramolecular organization are important issues whenever living beings are studied [1]. In addition to its considerable importance in life science, actin also serves as one of the few experimentally accessible model systems for semiflexible chain polymers [2, 3]. Globular actin monomers (G-actin) assemble into a two-stranded helical F-actin with a diameter of about 8 nm and a helical pitch of 37 nm. The contour length, L, of the filaments can be up to 100 μm. Previous measurements on unconfined actin filaments revealed a persistence length, L_P, of 8 - 25 μm [2, 3, 4, 5, 6, 7, 8, 9, 10]. F-actin is thus situated between stiff biopolymers (e.g. microtubules, $L_P \sim 5.2$ mm) and flexible biopolymers (e.g. DNA, $L_P \sim 50$ nm). Therefore, the properties of flexible, semiflexible, and stiff polymers can be investigated within a single experiment by adjusting the contour length. Since the contour length is within the range of optical resolution, fluorescently labelled actin filaments can be directly observed using optical microscopy. The physical properties of biopolymers are very challenging to investigate *in vivo* and the poor understanding of the mechanical details of the cytoskeleton further complicates the theoretical description of these systems [11, 12]. Therefore, extensive efforts have been made to model the cellular mechanics with purified reconstituted *in vitro* systems. In recent years, several experimental studies on freely fluctuating actin filaments in dilute solutions have been performed, elucidating some of the mechanical and statistical properties of these biopolymers [2, 3, 4, 5, 6, 7]. Considering the rather dense network of filamentous proteins within a eukaryotic cell (mesh size $\sim \mu$m), it is of substantial interest to regard the individual filament in an environment that resembles its native surrounding [13, 14]. In addition, investigations of biopolymers in confining geometry are important for

*Corresponding author. Electronic address: thomas.pfohl@ds.mpg.de

the fundamental understanding of the corresponding biological systems as well as for microfluidic applications in lab-on-a-chip platforms [15, 16, 17]. In this letter, we present investigations and analysis of thermal fluctuations of individual actin filaments confined in microchannels. We mimic the restraining network using microchannels with dimensions of about the same order of magnitude as the mesh size of the cytoskeleton. We use fluorescence microscopy to directly visualise thermal fluctuations of individual actin filaments in the microchannels and show that the mechanical and dynamic properties of the semiflexible polymers are strongly dependent on both the channel width, d, and filament length, L. The obtained tangent correlation of the filaments can be described by the worm like chain (WLC) model considering the confining potential of the channel walls as a parabolic potential.

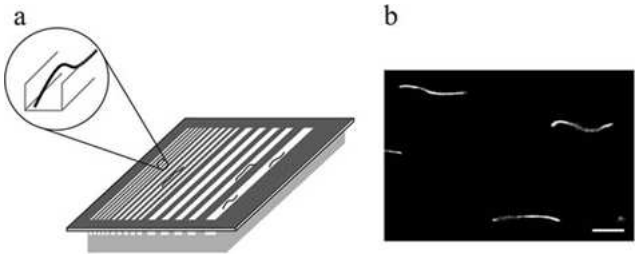

Figure 1: Experimental Setup. a) Sketch of the microchannel chamber with different channel widths, actin filaments are fluctuating in rectangular channels. b) Fluorescence micrograph (10 μm scale bar).

Experimental methods

Lyophilised rhodamine labelled G-actin was purchased from Cytoskeleton, Denver, USA. The powder was dissolved in ultrapure water to 10 mg/mL (in 5 mM tris(hydroxymethyl)aminomethane-hydrochloride (Tris-HCl) (pH 8.0), 0.2 mM NaATP, 0.2 mM $CaCl_2$, 5% sucrose, and 1% dextran), diluted in A-buffer (5 mM Tris-HCl (pH 8.0), 0.2 mM NaATP, 0.2 mM $CaCl_2$, 0.5 mM DTT, and 0.002% chlorhexidine) to 0.2 mg/mL and placed on ice for two hours to allow for depolymerisation of existing oligomers. Polymerisation buffer (100 mM Tris-HCl (pH 7.5), 20 mM $MgCl_2$, 500 mM KCl, and 10 mM ATP) was added to initiate the polymerisation process and the solution was incubated at room temperature for two hours (volume ratio A-buffer : polymerisation buffer = 9:1). The solution was diluted to a final monomer concentration of 70 nM in stabilisation buffer to prevent the actin filaments from depolymerising (A-buffer, polymerisation buffer (9:1), and 70 nM phalloidin). The solution was thoroughly mixed and kept at 4°C until it was used for the experiments. To avoid photobleaching and breakage of the filaments during observation, antifade solution (30 mM glucose, 10 mM DTT, 4 μM glucose oxidase, 0.2 mM NaATP, 5 mM Tris-HCl (pH 8.0), 2 mM CaCl, and 210 units/mL catalase) was added to the actin solution just before filling the microchannel chamber (volume ratio actin solution : antifade = 5:1). The microchannels were fabricated using standard soft lithography techniques [18, 19]. Briefly, SU-8 2 photo resist (Micro Resist Technology GmbH, Berlin, Germany) was spin coated onto a cleaned silicon wafer to a thickness of 1.4 μm. The coated wafers were then selectively exposed to UV light through a high resolution chrome mask and developed. The three dimensional structures (parallel channels, width d = 2, 4, 6 and 10 μm) were cast in PDMS, and these replicas were used for the experiments. The PDMS microstructures were plasma treated and irreversibly bound to glass cover slips which provides a tight seal. To avoid sticking of the actin filaments to the channel walls, the channel surfaces were coated with BSA (bovine serum albumin, 1 mg/mL) prior to filling the

chamber with the dilute F-actin solution. Van der Waals or electrostatic interactions between the filaments and the channel walls might still play a role. However, BSA coating of the channel walls was sucessfully used by several other groups and no influence on the fluctuations of the filaments was observed [3, 5]. We found that the filaments were fluctuating inside the channels without sticking for at least 24 h. Only data obtained from chambers with negligible flow rates which had no influence on the dynamics of the filaments were analysed. We observed the contour fluctuations of the biopolymers with an Olympus BX61 fluorescence microscope equipped with a 75 W Xenon lamp and a 100x Plan Apochromat oil immersion objective. Movies were recorded using a PCO SensiCamQE CCD camera (exposure time 100 ms, 10 frames per second). The microscopy images were binarised and skeletonised to a one-pixel-line using commercial image processing software (Image-Pro Plus, AnalySIS, MATLAB). To determine the tangent correlation, a smoothing spline fit was applied to the one-pixel-line. An arclength reparametrisation of the fitted line was obtained by dividing it into tangent vectors of equal length. The correlation of these tangent vectors as a function of the arclength, l, is given by their scalar product. An actin concentration of 70 nM was chosen to secure investigations of individual actin filaments avoiding interactions between actin filaments. We observed F-actin in a quasi-2D-system since the channels had a depth of merely 1.4 μm and the contour line of each filament was projected into the focal plane of the microscope. The width of the microchannels (2 to 10 μm) covered one order of magnitude, whilst their length (2 cm) guaranteed translational invariance in the direction of the channels (fig. 1). F-actin naturally has a polydisperse length distribution. Since we used a microfluidic chamber which included different channel widths (figure 1a), this allowed for the investigation of the channel width dependence and contour length dependence in a single experiment.

Results and discussion

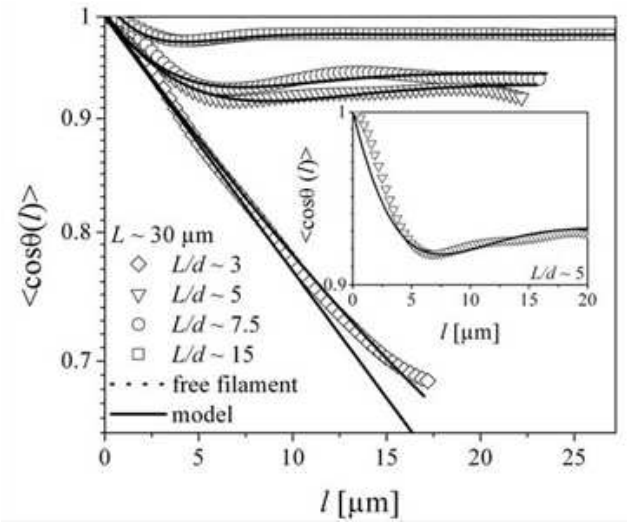

Figure 2: Channel width dependence of the tangent correlation of confined actin filaments; open symbols: experimental data; solid lines: theoretical model; dotted line: behavior of freely fluctuating ideal filaments. The symbol size corresponds to the error bars. Inset is a close up of the data and model for 6 μm channels.

Semiflexible polymers are best described by the worm-like chain (WLC) model [20, 21]. The basic idea is that the mechanical properties of the chain are completely

described by its bending energy $H = \frac{\kappa}{2}\int_0^L dl \left[\frac{\partial^2 \mathbf{r}(l)}{\partial l^2}\right]^2$, were κ is the bending rigidity of the filament and $\mathbf{r}$ is the position vector. By assuming a Boltzman distribution for these energies the exponentially decaying tangent correlation

$$\langle \cos\theta(l)\rangle \equiv \langle \overline{\mathbf{t}(s)\cdot\mathbf{t}(s+l)}\rangle = \exp\left(-l/2L_P\right) \tag{1}$$

for a 2D system may be obtained in a straightforward manner [20]. The factor 2 in the denominator of the exponent arises from the fact that the filament is confined to a two-dimensional plane [4, 5]. In addition to the spatial averaging within the same image (denoted by the bar in eq. 1), a time dependent averaging including all images of a movie was conducted. To further improve the statistics of our results, we also averaged the data of several filaments having the same contour length fluctuating in a channel of the same width. Our system showed $L_P = \kappa/k_BT = 19$ μm for unconfined filaments. In fig. 2, semi-logarithmic plots of the tangent correlations for fluctuating filaments in microchannels of different widths (2, 4, 6 and 10 μm) are shown. A minimum length of $L = 30$ μm was chosen for this analysis to assure that the contour length of the filaments was large compared to the channel widths d. The dotted line shows the tangent correlation for unconfined filaments (eq. 1) of persistence length $L_P = 19$ μm. Clearly, filaments confined in 10 μm channels ($L \sim 3\ d$) are not very strongly influenced by the channel geometry; they show almost the same behaviour as free filaments. However, for the smaller channels ($d \leq 6$ μm, $L \geq 5\ d$) a strong influence of the restraining channel walls is observed. We observe an overall increasing correlation with decreasing channel width. In addition, a local minimum is developed at l_{min}, followed by an oscillation about a saturation level which is finally reached for large l. For large l the correlation reaches a constant asymptotic value, instead of dropping to zero as for unconfined filaments. This asymptotic value increases with decreasing channel width, whereas the distance l_{min} decreases with decreasing channel width. These experimental results may be described by a modified WLC-model. While the model described above (eq. 1) is based only on the mechanical rigidity of the polymer, a second term accounting for the channel geometry was added. A first estimate is a parabolic wall potential $\frac{K}{2}z(l)^2$, where the z-axis is perpendicular to the direction of the channels and K is a constant value determining the strength of the potential. Naturally, higher orders in $z(l)$ have to be taken into account to exactly describe the geometry of the rectangular channels. However it turns out that we can describe our results quite well using this approximation. It is of great advantage that in this case the tangent correlation can be analytically solved:

$$\langle \cos\theta(l)\rangle = 1 - \frac{\lambda}{\sqrt{2}\,2L_P}\left(\cos\left(\frac{\pi}{4}\right) - \cos\left(\frac{\pi}{4}+\frac{l}{\lambda}\right)\exp\left(\frac{-l}{\lambda}\right)\right). \tag{2}$$

In addition to L_P this model uses a second fitting parameter, the deflection length, λ, which is characterised by the competition of bending energy and confining energy ($\lambda = (4\kappa/K)^{1/4}$). A descriptive idea of the deflection length and the appropriate scaling law $\lambda \propto L_P^{1/3} d^{2/3}$ has been introduced by Odijk [22]. Note that these scaling arguments, as well as more rigorous calculations of the deflection length were deduced for semiflexible filaments in cylindrical hard wall tubes of diameter d, whereas we used a parabolic potential to describe our system. However, the same scaling arguments can be obtained from the parabolic potential [23, 24]. In good agreement with the experimental results (see solid lines in figure 2), the tangent correlation (eq. 2) approaches a constant asymptotic non-zero value for large distances l:

$$\langle \cos\theta(l)\rangle \approx 1 - \frac{\lambda}{4L_P} = const. \neq 0. \tag{3}$$

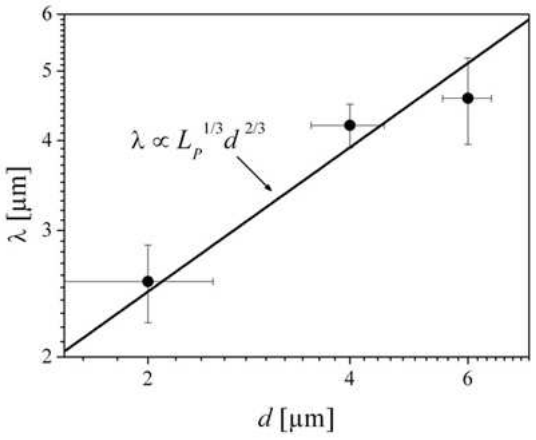

Figure 3: Dependence of the deflection length on the channel width d. The solid line marks $\lambda \propto L_P^{1/3} d^{2/3}$. The d error bars include slight differences in channel width as well as errors in the measurement of the width with a light microscope. The λ error bars stem from the error in l in the corresponding tangent-tangent correlation.

The ramification of this unique characteristic is that the tangential orientations of two polymer segments which are far apart from each other seem to be very well correlated (in contrast to the free tangent correlation where they are not correlated at all). This is however not a direct coupling of the segments as in the case of a stiffer polymer with a larger persistence length but all segments are coupled to the external channel potential. The external confining potential thus serves as a μm scale track for the polymer. Determining the position of the first local minimum of the modified tangent correlation (eq. 2) we find that it depends on the deflection length but not on the persistence length:

$$\lambda = \frac{2}{\pi} l_{min}. \tag{4}$$

In fig.3, the values for λ are plotted against the width of the channels. The solid line marks the scaling law $\lambda \propto L_P^{1/3} d^{2/3}$. The scaling law seems to be confirmed by our experimental results. In turn, the confining potential which is used plays an important role in setting λ as a characteristic length scale. A closer look at the initial slope of the tangent correlations, reveals deviations between the experimental results and the model. The inset in fig. 2 shows a close up of the data in direct comparison to the model (6 μm channels). We observe an initial zero-slope for our data, but a finite slope for the model curve. Consequently, there is a distinct deviation from the theoretical model for the data at small length scales ($l \leq 5$ μm). This effect is not due to the confining microchannels, since we also observe these deviations in measurements without channels (data not shown). Data on unconfined freely fluctuating filaments published by other groups show the same behaviour [3, 5]. To eliminate the possibility of a smear out of the short wavelength modes we compared different exposure times (25 and 200 ms) for unconfined filaments (data not shown). However, we did not observe a difference in the initial slope. The deviations might be due to an intrinsic non-linear stiffness of the filament chain, avoiding radii of curvature smaller than a certain minimum value. This feature could be taken into account by introducing a finite cut-off length, considering higher terms

in the bending energy [25]. Observation of the projection of the filaments' contour to the focal plane of the microscope instead of their 3D conformations might also lead to deviations on small length scales. In any case it is very challenging to draw a conclusion about the behaviour of the filaments on such small length scales where the experimental method (that is microscopy and confining channel) as well as the intrinsic mechanics of the filaments themselves may play a role.

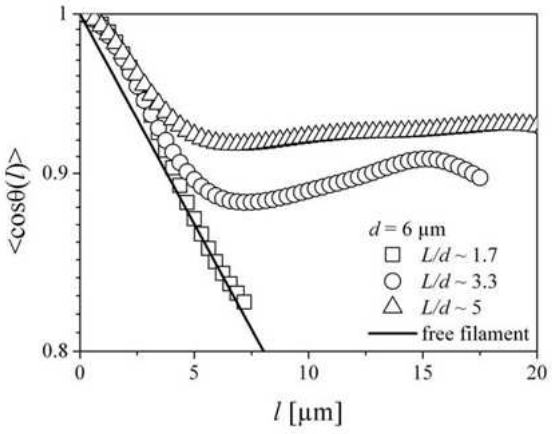

Figure 4: Contour length dependence of the tangent correlation of confined actin filaments. The black line marks the behavior for freely fluctuating ideal filaments. The symbol size corresponds to the error bars.

Data analysis can be conducted by varying the contour length whilst keeping the channel width constant. The data shown in fig. 4 display the tangent correlation of filaments with contour lengths of 10, 20, and 30 μm in 6 μm wide channels. As observed before (fig. 2), there is no influence of the channel walls discernible when channel width and contour length are in the same order of magnitude. However, for longer filaments the channel geometry does influence their tangent correlation in the same way as for varying channel widths. An overall increasing correlation with increasing contour length is observed. This dependence on the contour length of the filaments is not accounted for in existing theoretical descriptions. The WLC-model as well as the modified WLC-model assumes infinitely long filaments. A more quantitative description of the experimental results has to consider the finite length of the filaments.

Conclusions

In summary, we were able to observe single semiflexible actin filaments in microchannels using fluorescence microscopy. A strong dependence of the tangent correlation of the fluctuating filaments on the channel geometry and the filament length was found. The enhancement of the tangent correlation and their unique characteristics can be described using a modified WLC-model with a confining parabolic potential. A more quantitative description requires a more elaborate theoretical analysis incorporating the finite length of the filaments as well as an initial zero-slope of the tangent correlation. A better understanding and further investigations on the interplay of an individual filament and its surrounding is not only crucial for the comprehension of the mechanical properties of the cellar processes, but also for the behaviour of dilute polymer solutions in microfluidic applications.

Acknowledgments

We thank Erwin Frey, Klaus Mecke, Cyrus R. Safinya, Myung C. Choi, Youli Li and Dagmar Steinhauser for helpful discussions, and Ralph Müller and Alexander Otten for training in photolithography techniques. This project was supported by the DFG in the framework of the Emmy Noether Programme (PF 375/2).

References

[1] Alberts A., Bray D., Lewis J., Raff M., Roberts K. and Walter P. *Molecular Biology of the Cell*, Garland, New York, **2002**.

[2] Le Goff L., Hallatschek O., Frey E. and Amblard F. *Phys. Rev. Lett.* 89, **2002**, 258101.

[3] Ott A., Magnasco M., Simon A. and Libchaber A. *Phys. Rev. E* 48, **1993**, R1642.

[4] Gittes F., Mickey B., Nettelton J. and Howard J. *J. Cell Biol.* 120, **1993**, 923.

[5] Isambert H., Venier P., Maggs A.C., Fattoum A., Kassab R., Pantaloni D. and Carlier M.-F. *J. Biol. Chem.* 270, **1995**, 11437.

[6] Käs J., Strey H., Bärmann M. and Sackmann E. *Europhys. Lett.* 21, **1993**, 865.

[7] Käs J., Strey H., Tang J.X., Finger D., Ezzell R., Sackmann E. and Jamney P.-A. *Biophys. J.* 70, **1996**, 609.

[8] Yanagida T., Nakase M., Nishiyama K. and Oosawa F. *Nature* 307, **1984**, 58.

[9] Takebayashi T., Morita Y. and Oosawa F. *Biochim. Biophys. Acta* 492, **1977**, 375.

[10] Ishijima A., Doi T., Sakurada K. and Yanagida T. *Nature* 352, **1991**, 301.

[11] Howard J. *Mechanics of Motor Proteins and the Cytoskeleton* Sinauer, Sunderland **2001**.

[12] Boal D. *Mechanics of the Cell* Cambridge University Press **2002**.

[13] Pfohl T., Mugele F., Seemann R. and Herminghaus S. *ChemPhysChem* 4, **2003**, 1291.

[14] Wong I.Y., Gardel M.L., Reichman D.R., Weeks E.R., Valentine M.T., Bausch A.R. and Weitz D.A. *Phys. Rev. Lett.* 92, **2004**, 178101.

[15] Tegenfeldt J.O., Prinz C., Cao H., Chou S., Reisner W.W., Riehn R., Wang Y.M., Cox E.C., Sturm J.C., Silberzan P. and Austin R.H. *P. Natl. Acad. Sci. USA* 101(30), **2004**, 10979.

[16] Clemmens J., Hess H., Howard J. and Vogel V. *Langmuir* 19(5), **2003**, 1738.

[17] Bunk R., Klinth J., Montelius L., Nicholls I.A., Omling P., Tågerud S. and Månsson A. *Biochem. Bioph. Res. Co.* 301, **2003**, 783.

[18] Xia Y. and Whitesides G. *Ann. Rev. Mat. Sci.* 28, **1998**, 153.

[19] Delamarche E., Bernard A., Schmid H., Michel B., Biebuyck H. *Science* 276, **1997**, 779.

[20] Landau L.D. and Lifshitz E.M. *Statistical Physics* Pergamon Press, London **1958**.

[21] Kratky O. and Porod G. *Recl. Trav. Chim. Pay-B.* 68, **1949**, 1106.

[22] Odijk T. *Macromolecules* 16, **1983**, 1340.

[23] Kroy K. *Ph.D. thesis, TU München* **1998**.

[24] Hinner B., Tempel M., Sackmann E., Kroy K. and Frey E. *Phys. Rev. Lett.* 81, **1998**, 2614.

[25] Mecke K. *Private communications*, **2005**.